ISSN 0031-918X, Physics of Metals and Metallography, 2020, Vol. 121, No. 5, pp. 476–482. © Pleiades Publishing, Ltd., 2020.
Russian Text © The Author(s), 2020, published in Fizika Metallov i Metallovedenie, 2020, Vol. 121, No. 5, pp. 528–534.

STRUCTURE, PHASE TRANSFORMATIONS, AND DIFFUSION

Comparative Analysis of Structure and Properties of Quasibinary Al–6.5Cu–2.3Y and Al–6Cu–4.05Er Alloys

S. M. Amer[a], R. Yu. Barkov[a, *], O. A. Yakovtseva[a], and A. V. Pozdniakov[a]

[a] *National University of Science and Technology MISiS, Moscow, 119049 Russia*

**e-mail: barkov@misis.ru*

Received September 5, 2019; revised October 8, 2019; accepted October 18, 2019

Abstract—The evolution of the microstructure and mechanical properties of quasibinary Al–6.5Cu–2.3Y and Al–6Cu–4.05Er alloys during homogenization and subsequent thermomechanical treatment has been studied in this work. The Cu concentration in the aluminum solid solution increases during homogenization before quenching owing to the dissolution of a nonequilibrium excess of phases of crystallization origin and is 1.8 and 2.3% for the alloys containing Y and Er, respectively. The size of intermetallic phases in the Al–6.5Cu–2.3Y and Al–6Cu–4.05Er alloys homogenized at 605°C for 3 hours is 1.2 and 0.75 μm, respectively, and does not increase significantly with an increased annealing time. The Al–6Cu–4.05Er alloy is less prone to softening during annealing after rolling than the Y-containing alloy. This is explained by a greater degree of alloying of the aluminum solid solution (Al) and by a greater degree of dispersity of phases of crystallization origin. However, because of the same factor, the Er-containing alloy has a higher inclination to recrystallization and thereby a coarser recrystallized grain. As a result, the Al–6Cu–4.05Er alloy demonstrates higher mechanical tensile characteristics, especially after annealing at temperatures above 150°C.

Keywords: aluminum alloys, yttrium, erbium, microstructure, phase composition, mechanical properties

DOI: 10.1134/S0031918X20030023

INTRODUCTION

The alloy 1201 [1] (analogue of the american 2219 alloy [2]) is the only deformable alloy of the Al–Cu system that shows sufficiently high strength and heat resistance [2]. The main disadvantage of Al–Cu alloys is a high tendency to the formation of cracks of crystallization origin [3–5], which should be taken into account not only when preparing castings, but also ingots of deformed alloys. One of the main ways of improving manufacturability during casting is alloying with eutectic-forming elements, such as Si, Ni, Fe, and Mn [6]. However, a significant increase in casting characteristics can be achieved only at sufficiently high concentrations of additives, when coarse primary crystals are formed in the structure [6], which is undesirable for deformed alloys. It was shown in [7, 8] that the Al–4.5Cu–1.6Y and Al–4Cu–2.7Er alloys in the quasibinary sections Al–Al_8Cu_4Y and Al–Al8Cu4Er have a very narrow crystallization range, and the eutectic phases Al_8Cu_4Y and Al_8Cu_4Er are highly dispersed and possess thermal stability during homogenization before quenching. Despite the low solubility of yttrium and erbium in the aluminum solid solution, they are prone to the formation of dispersoids with an $L1_2$ structure during ingot annealing. This leads to an additional strengthening and an increase in the temperature of the onset of recrystallization, especially when zirconium and/or scandium are present in the alloy [9–15].

This work is aimed at a comparative analysis of the changes in the structure of Al–6.5Cu–2.3Y and Al–6Cu–4.05Er alloys with an enhanced eutectic fraction during homogenization and thermomechanical treatment.

EXPERIMENTAL

The Al–6.5Cu–2.3Y and Al–6Cu–4.05Er alloys were melted in a resistance furnace using pure Al (99.99%) and master alloys Al–53.5Cu, Al–8Y, and Al–8Er. The casting was carried out into a water-cooled copper mold with an internal cavity 40 mm wide, 20 mm thick, and 120 mm high. The cooling rate was approximately 15 K/s.

The heat treatment was performed using Nabertherm and SNOL furnaces with a fan with an accuracy of maintaining the temperature of 1 K. The heat-treated ingots were rolled at 440°C to a thickness of 10 mm and at room temperature to 1 mm.

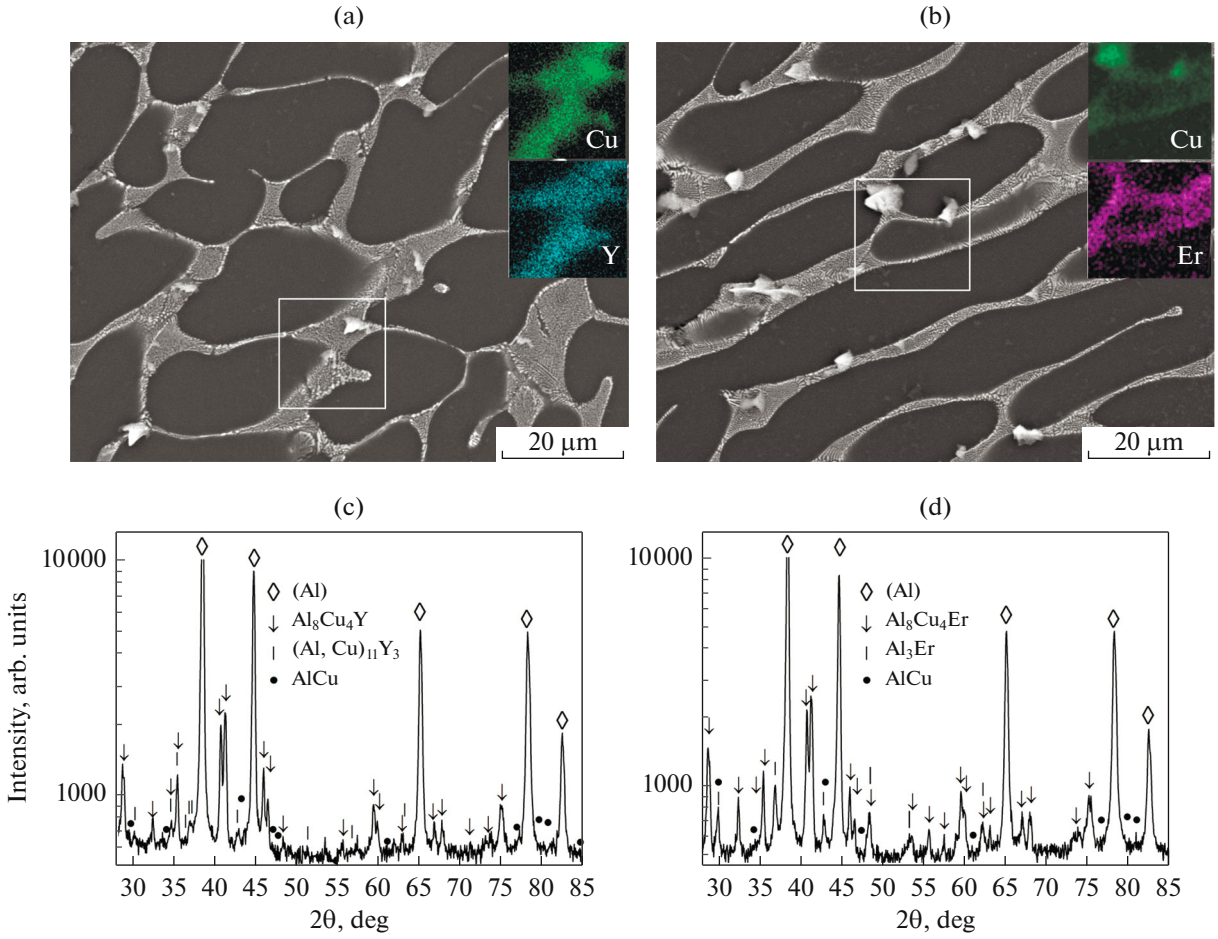

Fig. 1. (a, b) Microstructure (SEM images) and (c, d) X-ray diffraction patterns of as-cast (a, c) Al–6.5Cu–2.3Y and (b, d) Al–6Cu–4.05Er alloys.

The specimens for microstructural studies were prepared using a Struers Labopol-5 machine. The microstructural studies and phase identification were carried out using a Neophot 30 optical microscope (OM), a TESCAN VEGA 3LMH scanning electron microscope (SEM) equipped with an X-Max 80 energy dispersive detector, and a Bruker D8 Advance X-ray diffractometer. The substructure of foils was studied using a JEOL 2000-EX transmission electron microscope (TEM) at an operating voltage of 120 kV. The foils were prepared in a standard A2 electrolyte using a Struers Tenupol-5 electrolytic thinning machine. The liquidus and solidus temperatures were determined by a Labsys Setaram differential scanning calorimeter (DSC).

Hardness measurements were carried out using the standard Vickers method. The error did not exceed 3 HV. The tensile tests of samples made of 1-mm sheets were carried out using a Zwick/Roll Z250 All-round universal testing machine equipped with an automatic longitudinal strain gage.

RESULTS AND DISCUSSION

Figure 1 shows the microstructure and X-ray diffraction (XRD) patterns of as-cast Al–6.5Cu–2.3Y and Al–6Cu–4.05Er alloys. The as-cast microstructure is represented by aluminum solid-solution dendrites, dispersed eutectic, and coarser bright inclusions of crystallization origin. EDS analysis and elemental-distribution maps (insets in Figs. 1a, 1b) show that the bright phase is the AlCu compound, whose signals are presented in the XRD patterns (Figs. 1c, 1d). The dispersed eutectic consists of aluminum solid solution and Al_8Cu_4Y and Al_8Cu_4Er phases. These phases were also revealed previously in the less-alloyed Al–4.5Cu–1.6Y [7] and Al–4Cu–2.7Er [8] alloys. Dispersed inclusions of $(Al,Cu)_{11}Y_3$ and Al_3Er phases enriched in Y and Er, respectively, are present at the boundaries between the eutectic and the aluminum dendrites, which is also confirmed by previous studies [7, 8].

The calorimetric analysis showed that the liquidus and solidus temperatures for the Al–6.5Cu–2.3Y alloy are 635 and 615°C, respectively (Fig. 2a), and those for

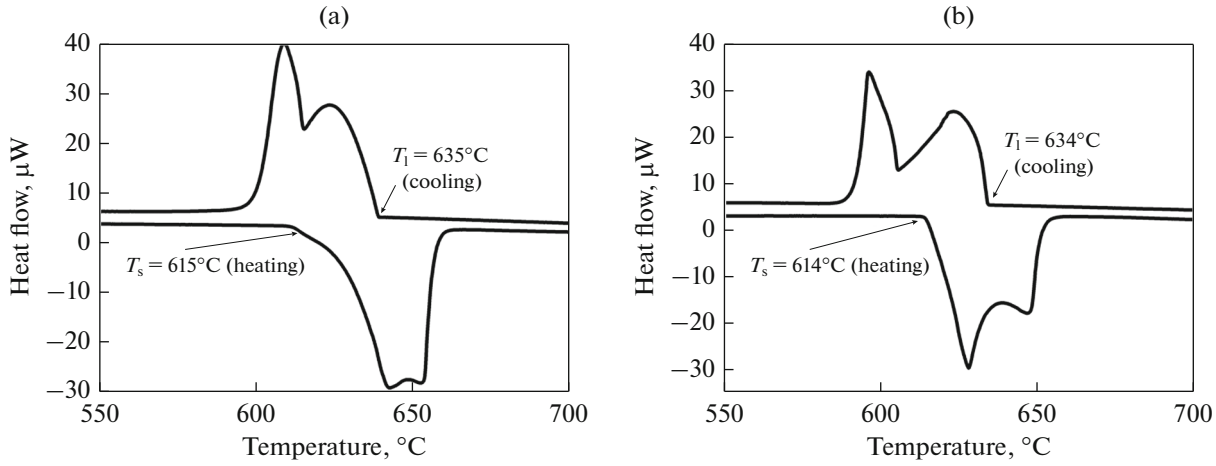

Fig. 2. DSC curves for (a) Al–6.5Cu–2.3Y and (b) Al–6Cu–4.05Er alloys.

the Al–6Cu–4.05Er alloy are 634 and 614°C, respectively (Fig. 2b). In accordance with the solidus temperatures of the studied alloys, the temperature of 605°C was chosen as the homogenization temperature before quenching.

The Al–6.5Cu–2.3Y and Al–6Cu–4.05Er alloys were subjected to homogenization annealing for 1, 3, and 6 hours with subsequent water quenching. The change in the microstructure (SEM images) during homogenization is presented in Fig. 3. Figure 4 shows the Cu concentration (in Al) and the size of excess phases as a function of the holding time of homogenization at 605°C. The annealing for 1 hour leads to a fragmentation and spheroidization of phases of crystallization origin; the mean size increases from 0.25 μm (Figs. 1a, 1b, and 4) to 1.2 and 0.75 μm in Al–6.5Cu–2.3Y and Al–6Cu–4.05Er alloys, respectively (Figs. 3a, 3b, and 4). In this case, the Cu concentration in the aluminum solid solution is seen in Fig. 4 to increase slightly. As the homogenization time increases, the phases of crystallization origin grow and the Cu concentration (in Al) increases. The latter is caused by the dissolution of nonequilibrium excess of phases of crystallization origin. However, the Cu concentration (2.3%, in Al) in the Al–6Cu–4.05Er alloy is seen (Fig. 4b) to exceed insignificantly the corresponding value for the Al–6.5Cu–2.3Y alloy (1.8%) and remains unchanged with increasing homogenization time from 3 to 6 hours. It should be noted that after a 3-hour annealing, the mean size of excess phases in the Al–6Cu–4.05Er alloy (1.3 μm) is smaller than that in the Al–6.5Cu–2.3Y alloy (1.9 μm) (Fig. 4). Therefore, the time of 3 hours was chosen for the homogenization before quenching, after which the ingots were rolled to sheets 1 mm thick.

Table 1. Recrystallized-grain size after annealing of sheets at 350, 450, and 550°C for 1 hour

Temperature, °C	Grain size, μm	
	Al–6.5Cu–2.3Y	Al–6Cu–4.05Er
350	7.8 ± 0.8	8.7 ± 0.9
450	9.8 ± 0.7	12.6 ± 0.6
550	11 ± 1	13 ± 1.2

Figure 5 shows the hardness of the alloys under study vs the temperature of annealing for 1 hour and the annealing time. The alloys are recrystallized in the range of 250–350°C (see insets in Figs. 5a, 5b). The Al–6Cu–4.05Er alloy is less prone to softening (Fig. 5b) in comparison with the Al–6.5Cu–2.3Y alloy (Fig. 5a), which is associated with a greater degree of alloying of the (Al) and with the presence of more dispersed phases of crystallization origin. However, for the same reason the Al–6Cu–4.05Er alloy has a higher stimulus to recrystallization and thereby a coarser recrystallized grain (Table 1). The hardness for these alloys after 1-hour annealing at temperatures above 350°C remains approximately unchanged.

At temperatures below 250°C, the softening (Figs. 5c, 5d) is caused by the processes of polygonization (Fig. 6). It should be noted that the hardness of the Al–6.5Cu–2.3Y alloy decreases more significantly, especially after annealing at 250°C. Figure 6e illustrates that the subgrain size in this alloy is significantly larger than 500 nm and exceeds the corresponding value (250 nm) for the Al–6Cu–4.05Er alloy

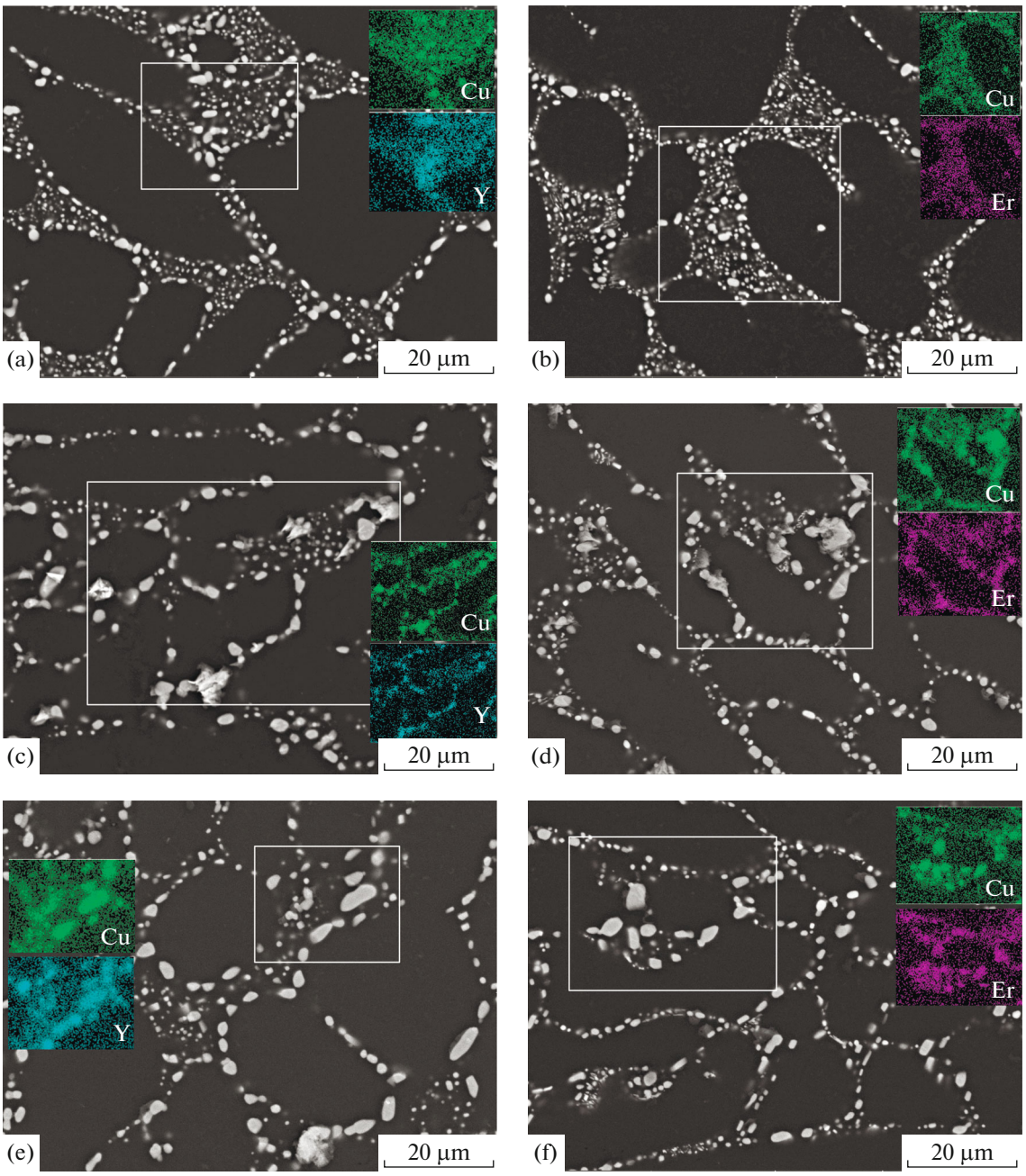

Fig. 3. Microstructure (SEM images) of (a, c, e) Al–6.5Cu–2.3Y and (b, d, f) Al–6Cu–4.05Er alloys after homogenization at 605°C for (a, b) 1, (c, d) 3, and (e, f) 6 h.

(Fig. 6f). After annealing at 100°C for 1 and 8 hours, a high density of dislocations still takes place, but a subgrain structure is formed (Figs. 6a–6d). In addition, the smaller subgrains are observed in the Al–6Cu–4.05Er alloy (Figs. 6b, 6d) rather than in the Al–6.5Cu–2.3Y alloy (Figs. 6a, 6c).

Table 2 shows that the Al–6Cu–4.05Er alloy possesses higher mechanical tensile properties, especially after annealing at temperatures above 150°C. At the same time, the plasticity of both the studied alloys is less than 5% (Table 2), which is most likely due to the higher fraction of phases of crystallization origin in the structure, since the relative plasticity is slightly higher in the less alloyed alloys [7, 8]. The plasticity of the Al–6.5Cu–2.3Y and Al–6Cu–4.05Er alloys after annealing at 250 and 300°C, respectively, increases to 13–14%. However, the yield stress sharply decreases

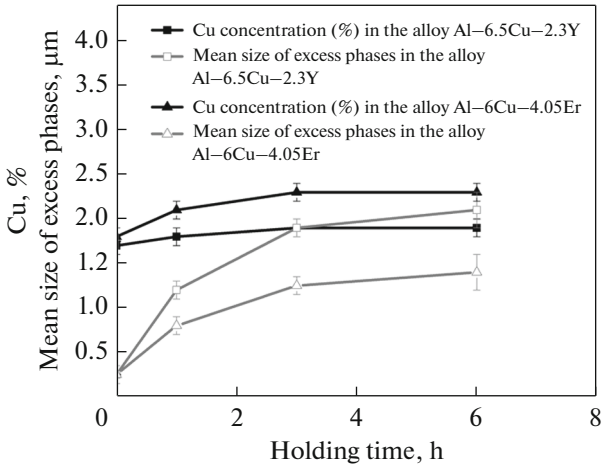

Fig. 4. Copper concentration in (Al) and size of excess phases as a function of holding time upon homogenization before quenching from 605°C.

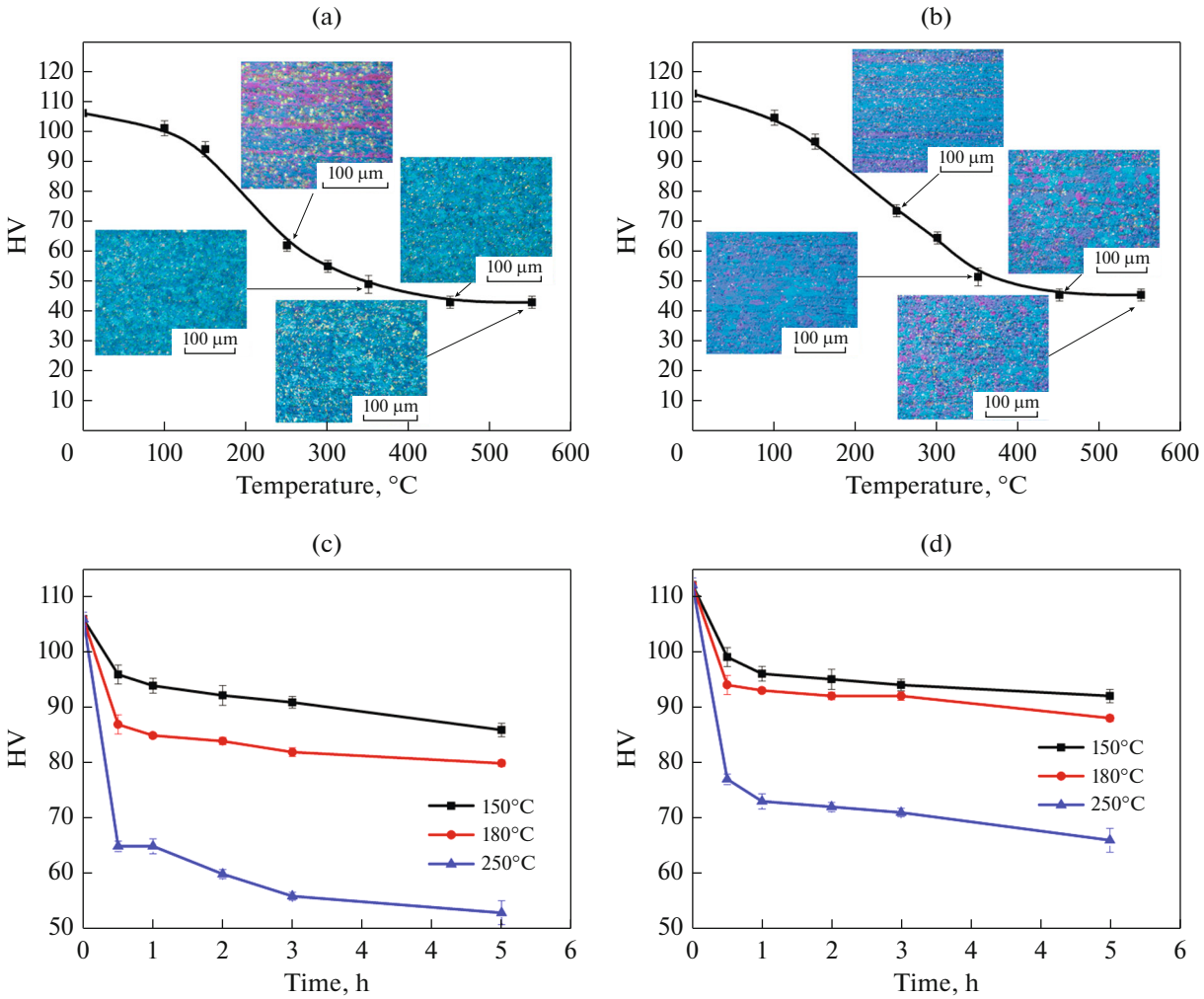

Fig. 5. Hardness vs (a, b) 1-h annealing temperature and (c, d) annealing time for (a, c) Al–6.5Cu–2.3Y and (b, d) Al–6Cu–4.05Er alloys.

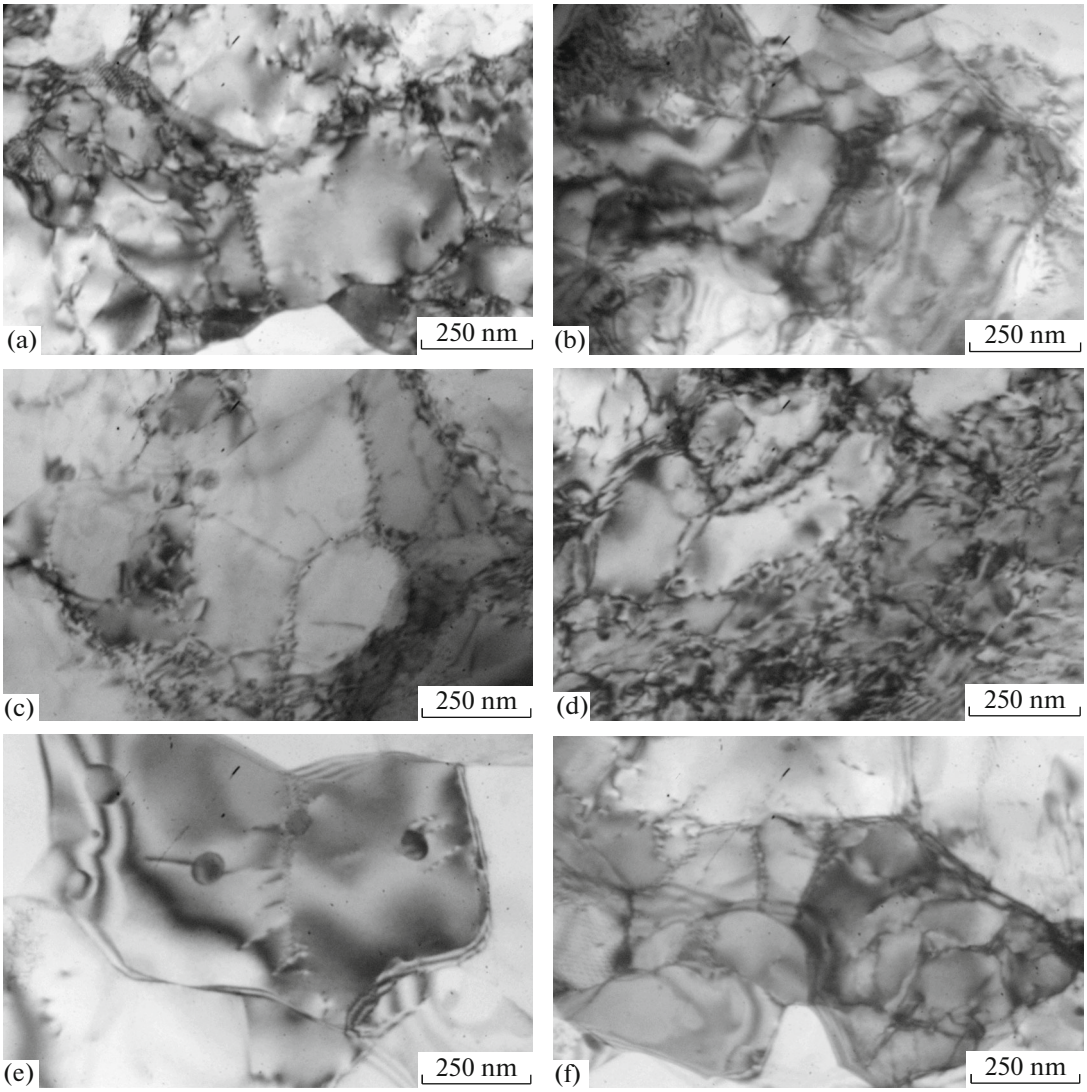

Fig. 6. Substructure (TEM images) of (a, c, e) Al–6.5Cu–2.3Y and (b, d, f) Al–6Cu–4.05Er alloys after annealing at 100°C for (a, b) 1 and (c, d) 8 hours and at 250°C for (e, f) 0.5 hours.

(from 254–282 MPa to 191–198 MPa), which, as is shown above, is caused by the growth of subgrains at 250°C.

CONCLUSIONS

A comparative analysis of the evolution of the microstructure and mechanical properties of the quasibinary Al–6.5Cu–2.3Y and Al–6Cu–4.05Er alloys in the process of the homogenization annealing and subsequent thermomechanical treatment has been carried out. Owing to the dissolution of the nonequilibrium excess of phases of crystallization origin during the homogenization, the Cu concentration in the aluminum solid solution increases and is 1.8 and 2.3% for the alloys containing Y and Er, respectively. The size of intermetallic phases in the Al–6.5Cu–2.3Y and Al–6Cu–4.05Er alloys homogenized at 605°C for 3 hours is 1.2 and 0.75 μm, respectively. The Al–6Cu–4.05Er alloy is less prone to softening than the Y-containing alloy. This is explained by a greater degree of alloying of the (Al) and by the presence of more dispersed phases of crystallization origin. However, because of the same factor, the Er-containing alloy has a higher stimulus to recrystallization and thereby a coarser recrystallized grain. As a result, the Al–6Cu–4.05Er alloy demonstrates higher mechanical tensile properties, especially after annealing at temperatures above 150°C.

Table 2. Mechanical tensile properties of alloys after thermomechanical treatment

State	$\sigma_{0.2}$, MPa	σ_u, MPa	δ, %
Al–6.5Cu–2.3Y			
Deformed state	294 ± 1	333 ± 2	3.6 ± 0.2
Annealing at 100°C for 1 h	277 ± 1	319 ± 1	1.6 ± 0.1
Annealing at 100°C for 3 h	277 ± 3	313 ± 1	3.0 ± 0.8
Annealing at 100°C for 8 h	271 ± 2	306 ± 1	3.6 ± 0.6
Annealing at 150°C for 1 h	257 ± 2	284 ± 1	2.1 ± 0.9
Annealing at 150°C for 3 h	254 ± 1	273 ± 1	2.2 ± 0.4
Annealing at 250°C for 0.5 h	198 ± 3	203 ± 1	13.2 ± 0.9
Al–6Cu–4.05Er			
Deformed state	298 ± 2	335 ± 4	3.5 ± 0.3
Annealing at 100°C for 1 h	282 ± 1	318 ± 2	3.1 ± 0.7
Annealing at 100°C for 3 h	278 ± 3	312 ± 1	2.8 ± 0.4
Annealing at 100°C for 8 h	278 ± 1	313 ± 1	4.4 ± 0.8
Annealing at 150°C for 1 h	273 ± 2	302 ± 2	2.8 ± 0.9
Annealing at 150°C for 3 h	267 ± 2	289 ± 3	2.8 ± 0.7
Annealing at 250°C for 0.5 h	225 ± 1	234 ± 2	3.1 ± 1.2
Annealing at 300°C for 10 min	191 ± 1	212 ± 1	14.4 ± 0.6

FUNDING

The work was supported by the Russian Science Foundation (project no. 19-79-10242).

REFERENCES

1. *GOST 1583-93. Casting Aluminum Alloys. Technical Conditions* (IPK Izd-vo standartov, Minsk, 2000) [in Russian].
2. *ASM Handbook. Properties and Selection: Nonferrous Alloys and Special-Purpose Materials. Vol. 2* (The Materials Information Company, 2010).
3. I. I. Novikov, *Hot Brittleness of Nonferrous Metals and Alloys* (Nauka, Moscow, 1966) [in Russian].
4. D. G. Eskin, Suyitno, and L. Katgerman, "Mechanical properties in the semi-solid state and hot tearing of aluminium alloys," Prog. Mater. Sci. **49**, 629–711 (2004).
5. V. S. Zolotorevskiy and A. V. Pozdniakov, "Determining the hot cracking index of Al–Si–Cu–Mg casting alloys calculated using the effective solidification range," Int. J. Cast Met. Res. **27**, 193–198 (2014).
6. V. S. Zolotorevskiy, A. V. Pozdniakov, and A. Yu. Churyumov, "Search for promising compositions for developing new multiphase casting alloys based on Al–Cu–Mg matrix using thermodynamic calculations and mathematic simulation," Phys. Met. Metallogr. **113**, 1052–1060 (2012).
7. A. V. Pozdniakov and R. Y. Barkov, "Microstructure and materials characterisation of the novel Al–Cu–Y alloy," Mater. Sci. Technol. **34**, 1489–1496 (2018).
8. A. V. Pozdnyakov, R. Y. Barkov, Z. Sarsenbaev, S. M. Amer, and A. S. Prosviryakov, "Evolution of microstructure and mechanical properties of a new Al–Cu–Er wrought alloy," Phys. Met. Metallogr. **120**, 614–619 (2019).
9. Y. Zhang, K. Gao, S. Wen, H. Huang, Z. Nie, and D. Zhou, "The study on the coarsening process and precipitation strengthening of Al3Er precipitate in Al–Er binary alloy," J. Alloys Compd. **610**, 27–34 (2014).
10. S. P. Wen, K. Y. Gao, Y. Li, H. Huang, and Z. R. Nie, "Synergetic effect of Er and Zr on the precipitation hardening of Al–Er–Zr alloy," Scr. Mater. **65**, 592–595 (2011).
11. S. P. Wen, K. Y. Gao, H. Huang, W. Wang, and Z. R. Nie, "Precipitation evolution in Al–Er–Zr alloys during aging at elevated temperature," J. Alloys Compd. **574**, 92–97 (2013).
12. A. V. Pozdniakov, R. Y. Barkov, A. S. Prosviryakov, A. Y. Churyumov, I. S. Golovin, and V. S. Zolotorevskiy, "Effect of Zr on the microstructure, recrystallization behavior, mechanical properties and electrical conductivity of the novel Al–Er–Y alloy," J. Alloys Compd. **765**, 1–6 (2018).
13. Y. Zhang, H. Gao, Y. Kuai, Y. Han, J. Wang, B. Sun, S. Gu, and W. You, "Effects of Y additions on the precipitation and recrystallization of Al–Zr alloys," Mater. Charact. **86**, 1–8 (2013).
14. Y. Zhang, J. Gu, Y. Tian, H. Gao, J. Wang, and B. Sun, "Microstructural evolution and mechanical property of Al–Zr and Al–Zr–Y alloys," Mater. Sci. Eng., A **616**, 132–140 (2014).
15. A. V. Pozdniakov, R. Yu. Barkov, S. M. Amer, V. S. Levchenko, A. D. Kotov, and A. V. Mikhaylovskaya, "Microstructure, mechanical properties and superplasticity of the Al–Cu–Y–Zr alloy," Mater. Sci. Eng., A **758**, 28–35 (2019).

Translated by O. Golosova